
Shortened PET Data Acquisition Protocol for the Quantification of ^{18}F -FDG Kinetics

Ludwig G. Strauss, MD; Antonia Dimitrakopoulou-Strauss, MD; and Uwe Haberkorn, MD

Medical PET Group, Biological Imaging, Clinical Cooperation Unit Nuclear Medicine, German Cancer Research Center, Heidelberg, Germany

A modified short dynamic protocol was defined and evaluated to predict kinetic parameters of ^{18}F -FDG metabolism from a dynamic data acquisition. **Methods:** The evaluation included 151 datasets obtained from 60 patients examined with ^{18}F -FDG and a dynamic data acquisition protocol of 60 min. Standardized uptake values (SUVs) were calculated for the individual time frames, and a 2-compartment model was applied to the data. The kinetic parameters and the ^{18}F -FDG influx, calculated from the model data, served as the reference for the analysis. Correlation was analyzed for the SUVs and the reference data. Subset analysis identified time intervals that can be used to predict the reference parameters based on a second-order polynomial function. **Results:** Significant correlations were noted for SUVs and ^{18}F -FDG influx, vascular fraction (VB), and the rate constant k_1 . The influx was associated mainly with SUVs of late acquisition times, whereas higher correlations were noted for early acquisition intervals and VB, as well as k_1 . A short dynamic acquisition protocol was defined on the basis of a short dynamic sequence 1–10 min after tracer injection and a static acquisition 56–60 min after tracer application. The correlation coefficients exceeded 0.9 for influx, VB, and k_1 when the SUVs of the input area (blood) and the target area were used to predict the kinetic parameters. **Conclusion:** A short dynamic data acquisition protocol can be used to obtain more detailed information about ^{18}F -FDG kinetics. The results demonstrate that ^{18}F -FDG influx, VB, and k_1 can be estimated with high accuracy from SUVs.

Key Words: ^{18}F -FDG; quantification; PET

J Nucl Med 2003; 44:1933–1939

PET with ^{18}F -FDG is frequently used for oncologic and nononcologic applications to assess tissue viability. Although simple visual evaluation is most common for routine PET studies, interest in a more quantitative approach is increasing. One parameter for the quantitative evaluation is based on the normalization of tracer concentrations for the injected dose and body weight, for which the term *stan-*

darized uptake value (SUV) was introduced more than 13 y ago (1). However, the ^{18}F -FDG uptake 1 h after tracer injection is the result of a dynamic process. Therefore, dynamic measurements are the most accurate approach to quantify ^{18}F -FDG kinetics. Although static measurements 1 h after tracer injection reflect the global ^{18}F -FDG accumulation at a single time point, more information is provided with dynamic data acquisitions.

Several attempts have been made to reduce the complexity of dynamic data acquisition, which demands more time for the data acquisition and also more sophisticated software for the data evaluation than does a simple static measurement. Matthies et al. performed dual-point measurements on patients with pulmonary nodules and found a high sensitivity (100%) for the detection of malignant tumors, whereas the specificity was 89% (2). Hubner et al. compared visual evaluation, SUV, and Patlak analysis in patients with malignant lung lesions and reported that accuracy improved when both SUV and Patlak values were used for the evaluation (3).

Gupta et al. performed ^{18}F -FDG studies on patients with malignant lung and mediastinal lesions and noted that, in patients with borderline SUVs, kinetic data may provide further help in differentiating the lesions (4). Dimitrakopoulou-Strauss et al. used dynamic PET studies in patients with soft-tissue sarcomas and evaluated the impact on diagnosis and the correlation to grading (5). The authors noted some overlap when SUVs were used to differentiate benign from malignant lesions. Furthermore, SUV was helpful to identify grade III tumors, but use of the full kinetic information permitted differentiation of further classes. The authors concluded that evaluation of the full ^{18}F -FDG kinetics is necessary for these tumors and is superior to a single static data acquisition (5). Similar results were reported by Nieweg et al., who showed a correlation between metabolic rate and tumor grade in soft-tissue sarcomas (6).

Besides being applied for diagnostic purposes, dynamic PET has been used to evaluate chemotherapeutic effects. Using SUV and Patlak analysis, Römer et al. assessed changes in ^{18}F -FDG metabolism in patients receiving chemotherapy because of Non-Hodgkin's lymphoma (7). The authors emphasized that "in NHL, dynamic acquisition combined with Patlak analysis of FDG kinetics may provide

Received Apr. 11, 2003; revision accepted Aug. 14, 2003.
For correspondence or reprints contact: Ludwig G. Strauss, MD, Medical PET Group, Biological Imaging (E060-1), Clinical Cooperative Unit Nuclear Medicine, German Cancer Research Center, Im Neuenheimer Feld 280, D-69120 Heidelberg, Germany.
E-mail: lgs@ads-lgs.com

superior information in therapy monitoring.” These results support the use of dynamic data acquisition, especially for evaluating therapeutic effects.

The literature data direct to the combined evaluation of PET studies, based on visual assessment as well as on a quantitative approach. In particular, the analysis of tracer kinetics based on the Patlak approach or compartment modeling provides superior information. The major limitation of both methods is the 1-h dynamic data acquisition and the requirement of an input function for the quantification of ^{18}F -FDG kinetics. Ohtake et al. showed that the arterial input function can be replaced by image-derived data (8). However, the dynamic data acquisition for 1 h prolongs the overall scanning time significantly and can produce difficulties with scanning time if a whole-body scan is needed in addition to the dynamic acquisition.

The primary aim of the study was to investigate if a short acquisition protocol yields information about ^{18}F -FDG kinetics exceeding the information based on SUV. For this purpose, we compared the ^{18}F -FDG kinetic data derived from a 60-min full dynamic acquisition with those obtained from a modified, short acquisition protocol. A main aim was to reduce the number of frames for the data acquisition in order to achieve a protocol suitable for routine application. The classic 2-compartment model was used as the reference, and the following parameters were calculated: vascular fraction (VB), rate constants k_1 – k_4 , and ^{18}F -FDG influx, which was calculated from the compartment data. We identified the contribution of the SUVs for the individual time frames of the dynamic ^{18}F -FDG study to the quantification parameters. Based on the results, we propose a simplified method for the prediction of quantitative parameters.

MATERIALS AND METHODS

The study included 151 dynamic datasets obtained from 60 oncologic patients referred for ^{18}F -FDG PET examinations for primary tumor diagnostics or evaluation after chemotherapy. The histology comprised 24 bone tumors, 14 colorectal carcinomas, 7 non-small cell lung tumors, 7 soft-tissue sarcomas, 4 breast carcinomas, and 4 patients with liver metastases from colorectal carcinoma. Tumor and scar tissue (if available) was included in the evaluation to cover a wide range of uptake data. Dynamic PET studies were performed for 60 min after the intravenous application of 300–370 MBq ^{18}F -FDG using a 23-frame protocol (10 frames of 1 min, 5 frames of 2 min, and 8 frames of 5 min). A dedicated PET system (ECAT EXACT HR+; Siemens Co.) with an axial field of view of 15.3 cm, operated in septa-extended (2-dimensional) mode, was used for patient studies. The system allowed the simultaneous acquisition of 63 transverse slices with a theoretic slice thickness of 2.4 mm. For attenuation correction of the acquired emission tomographic images, transmission scans were obtained for a total of 10 min before the radionuclide was applied. All PET images were attenuation corrected, and an image matrix of 256×256 pixels was used for iterative image reconstruction. The reconstructed images were converted to SUV images on the basis of the following formula (1): $\text{SUV} = \text{tissue concentration (Bq/g)} / (\text{injected dose [Bq]} / \text{body weight [g]})$.

The dynamic PET data were evaluated using the software package PMod (University of Zurich) (9,10). Hypermetabolic areas on the transaxial, coronal, and sagittal images were evaluated visually. Time-activity curves were created using volumes of interest (VOIs). A VOI consisted of several regions of interest (ROIs) over the target area. Irregular ROIs were drawn manually. To compensate for possible patient motion during the acquisition, the original ROIs were visually repositioned but not redrawn. A detailed quantitative evaluation of tracer kinetics requires the use of compartment modeling. A 2-tissue-compartment model is the standard methodology for the quantification of dynamic ^{18}F -FDG studies (11,12). We use the term *target* for the VOI of a space-occupying lesion (e.g., tumor or scar) and the term *input* for the VOI of an arterial vessel. So as not to cover only a small group of tumors with high ^{18}F -FDG uptake, both tumors with high metabolic activity and scar tissue were included in the evaluation.

One problem in patient studies is accurate measurement of the input function, which theoretically requires arterial blood sampling. However, the input function can be retrieved from the image data with good accuracy (8). For the input function, the mean value of the VOI data obtained from a large arterial vessel, such as the descending aorta, was used. A vessel VOI consisted of at least 7 ROIs in sequential PET images. The descending aorta was preferentially used for this purpose, because the spillover from other organs is low and the descending aorta extends from the upper chest to the lower abdomen. The recovery coefficient is 0.85 for a diameter of 8 mm and for the system described above. To avoid spillover from the myocardium, we did not use VOIs of the heart for the input function. Noise in the input curve affects the parameter estimates. Therefore, we used a preprocessing tool, available in the PMod software, which allows a fit of the input curve, namely by a sum of up to 3 decaying exponentials, to reduce noise. k_1 – k_4 were calculated using a 2-compartment model implemented in the PMod software, taking into account the VB in a VOI as an additional variable. Details about the applied compartment model are described by Burger and Buck (9). One major advantage of the PMod software is the graphical interface, which allows interactive configuration of the kinetic model by the user and applies some preprocessing steps, such as setting up initial values and limits for the fit parameters. Each plot was evaluated visually for quality of fit. Each model curve was compared with the corresponding time-activity curve, and the total summed squares (X^2) difference was used as the cost function, where the criterion was to minimize the X^2 of the differences between the measured and the model curve (X^2 was usually less than 1). This means that the squared residuals (measured value minus estimated value) are multiplied by weights. In theory, the weight should be related to the SE of a measurement. The distribution at each individual point is taken to be gaussian, with an SD to be specified. The residual covariance was dependent on the kinetic parameter and typically less than 10% for k_1 . The model parameters were accepted when k_1 – k_4 was less than 1 and the VB values exceeded 0. The unit for k_1 – k_4 is 1/min, whereas VB reflects the fraction of blood within the evaluated volume. After compartment analysis, we calculated the global influx of ^{18}F -FDG from the compartment data using the following formula: $\text{influx} = (k_1 \times k_3) / (k_2 + k_3)$.

Statistical analysis was performed using the Statistica software package (version 6.0; StatSoft Co.) on a personal computer (Pentium IV [Intel Corp.], 1.8 GHz, 512 MB RAM) running with Windows XP professional (Microsoft Co.). First, a linear correlation analysis was performed for the SUV of each individual time

frame and the kinetic parameters of the 2-compartment model, which served as the reference. Then, best-subset analysis was used to select those acquisition intervals that were most suitable to predict the influx and the kinetic constants obtained by the 2-compartment analysis. The second demand was that the data acquisition be confined to a maximum of 2 short dynamic or static acquisitions to achieve a protocol that can be used routinely for patient examinations. Based on the subset analysis, a second-order polynomial regression function was fitted to the SUV of the selected time frames in order to accurately predict the kinetic parameters and the influx.

RESULTS

The 56- to 60-min SUV was highly variable, with a range of 0.11–10.44 (median: 1.66). The correlation coefficients of the target area SUVs for the individual acquisition intervals with the ^{18}F -FDG influx and the rate constants of the compartment model are presented in Table 1. The correlation coefficient for the SUV of each individual time frame and the ^{18}F -FDG influx exceeded 0.7 for acquisition times later than 20 min (Table 1). The highest correlation was obtained for the SUV of the time interval 56–60 min after injection and influx (Table 1). Generally, influx correlated with acquisition times longer than 1 min, and the correlation

TABLE 1
Correlation Coefficients for SUV and Parameters
of ^{18}F -FDG Kinetics

Minutes	VB	k1	k2	k3	k4	Influx
1	0.63	0.46	0.13	-0.06	-0.18	0.13
2	0.65	0.63	0.13	-0.06	-0.15	0.32
3	0.67	0.69	0.14	-0.06	-0.15	0.32
4	0.66	0.68	0.12	-0.05	-0.16	0.36
6	0.66	0.66	0.07	-0.02	-0.15	0.41
6	0.66	0.68	0.05	-0.03	-0.15	0.45
7	0.62	0.63	0.03	-0.03	-0.15	0.46
8	0.60	0.61	0.01	-0.01	-0.15	0.50
9	0.59	0.59	-0.02	-0.01	-0.16	0.53
10	0.59	0.57	-0.04	0.00	-0.14	0.54
11–12	0.60	0.57	-0.07	0.01	-0.15	0.58
13–14	0.59	0.57	-0.04	0.03	-0.15	0.62
15–16	0.56	0.55	-0.05	0.04	-0.15	0.65
17–18	0.56	0.55	-0.02	0.06	-0.16	0.66
19–20	0.53	0.51	-0.06	0.07	-0.16	0.68
21–25	0.52	0.50	-0.07	0.09	-0.16	0.71
26–30	0.49	0.51	-0.02	0.11	-0.17	0.72
31–35	0.48	0.48	-0.03	0.12	-0.18	0.74
36–40	0.47	0.49	-0.01	0.14	-0.18	0.75
41–45	0.46	0.46	-0.03	0.14	-0.18	0.75
46–50	0.44	0.44	-0.03	0.13	-0.19	0.75
51–55	0.43	0.45	-0.02	0.13	-0.19	0.75
56–60	0.43	0.45	-0.02	0.14	-0.21	0.75

The following kinetic parameters were assessed: VB, k1–k4, and influx for each individual acquisition interval. All correlation coefficients for VB and k1 are significant on $P < 0.01$ level. Correlation coefficients for influx are significant for 2–60 min. Although influx was correlated mainly with late acquisition times, VB and k1 were correlated with early acquisition times.

coefficients were significant ($P < 0.01$) for 2–60 min after tracer injection. In contrast, the highest correlation coefficients were observed for SUV, VB, and k1 for acquisition times less than 10 min after tracer injection. All correlation coefficients for SUV, VB, and k1 were significant on the $P < 0.01$ level for 1–60 min after tracer application. No significant correlation was observed for SUV and the constants k2–k4.

Best-subset analysis was used to select those frames that were best suited for prediction of the kinetic parameters, based on a limited number of PET acquisition frames. On the basis of the subset analysis, we defined a short acquisition protocol consisting of a dynamic acquisition of ten 1-min frames and a late static image 56–60 min after tracer injection. Regression functions, using a second-order polynomial, were calculated using the SUVs of the selected time frames of the dynamic series as independent variables and using the parameters influx, VB, and k1 as dependent variables. Functions were calculated for the combined use of input and target data, for the use of target data alone, and for the use of a summed 10-min image for the input and target region together with a 56- to 60-min image for the target area (Table 2). Using the input data for 1–10 min, the data for a target area from 1 to 10 min, and the data for a target area from 56 to 60 min, a correlation coefficient of 0.9028 was achieved for the ^{18}F -FDG influx (Table 2). The correlation was lower ($r = 0.8520$) when only the data for the target area were used to predict the influx (Table 2). The easiest procedure was the acquisition of one 10-min frame immediately after tracer injection and a second 5-min frame at 56–60 min. The correlation coefficient was 0.8302 for this procedure.

A correlation coefficient of 0.9195 was found for VB when the input (1–10 min) and target data (1–10 min and 56–60 min) were used (Table 2). The correlation coefficient decreased to 0.7484 when only the data of the target area were used to estimate the parameter. The use of a summed 1- to 10-min frame for both the input and the target area, as well as a late frame 56–60 min after injection for the target region, resulted in a low correlation coefficient of 0.7974.

k1 showed the highest correlation coefficient, with $r = 0.9305$ when both the input and target data were used (Table 2). The correlation coefficient was 0.8084 when only the target data for 1–10 min and 56–60 min after injection were used. The use of the SUV of a summed image for 1–10 min and the SUV of a late image for 56–60 min resulted in a low correlation coefficient of 0.8424.

A scatter diagram of the best results for VB, k1, and influx are shown in Figures 1–3.

DISCUSSION

One important aspect of PET is the possibility of performing highly accurate, noninvasive quantitative measurements of tracer concentration in patients. Because of the high sensitivity, even positron-emitting radionuclides gen-

TABLE 2

Prediction of Influx, Vessel Density, and k1 from SUV

Parameter	Input + target	Target	Summed image
Influx	0.9028	0.8520	0.8302
VB	0.9195	0.7484	0.7974
k1	0.9305	0.8084	0.8424

Data are correlation coefficients for polynomial regression function (second order) using SUV data as independent variables and influx, VB, or k1 as dependent variable. All correlation coefficients are significant for $P < 0.01$. Best results were obtained for influx, VB, and k1 when both dynamic data of input region and target area were used to estimate parameters. Input + target = SUVs 1–10 min for input area and 1–10 min as well as 56–60 min for target area; target = SUVs 1–10 and 56–60 min for target area; summed image = summed 10-min image (1–10 min) for input area and summed 10-min image (1–10 min) as well as 56–60 min for target area.

erated during radiotherapy can be measured (13). In an experimental study, Haberkorn et al. showed that quantitative analysis of ^{18}F -FDG kinetics provided information about biologic processes and that ^{18}F -FDG kinetics were dependent on the expression of glycolysis-associated genes (14). The use of a 2-compartment model is generally accepted to assess the kinetics of ^{18}F -FDG. Twenty years ago, Sokoloff and Smith provided solutions for the application of the ^{18}F -FDG model and reported the rate constants (12). Limited studies were performed on humans to assess the rate constants in malignant tumors.

Quantitative dynamic PET ^{18}F -FDG studies were performed by Dimitrakopoulou-Strauss et al. on patients with bone lesions (15). The authors used compartment modeling,

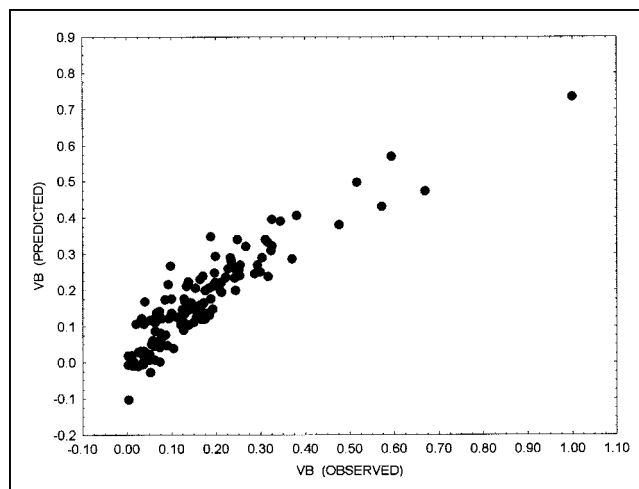


FIGURE 2. Correlation of VB as calculated by 2-compartment model (VB [observed]) and predicted VB (VB [predicted]) using short acquisition protocol. Input data from 1 to 10 min (10 frames) and target area from 1 to 10 min (10 frames) and from 56 to 60 min (1 frame) were used for prediction, based on polynomial function (degree 2) for data fitting. Correlation coefficient of 0.9195 was obtained.

noncompartment modeling, and simple static uptake measurements to analyze the data. They applied the Bayesian analysis to their results and showed that best results were obtained with full compartment modeling. Wu et al. evaluated the SUV and metabolic rate in bone lesions (16). When a cutoff of 1.8 of the average SUV was used, the sensitivity and specificity for discrimination of malignancy from benign disease were 85% and 82.4%, respectively. The metabolic rate for ^{18}F -FDG showed a comparable sensitivity

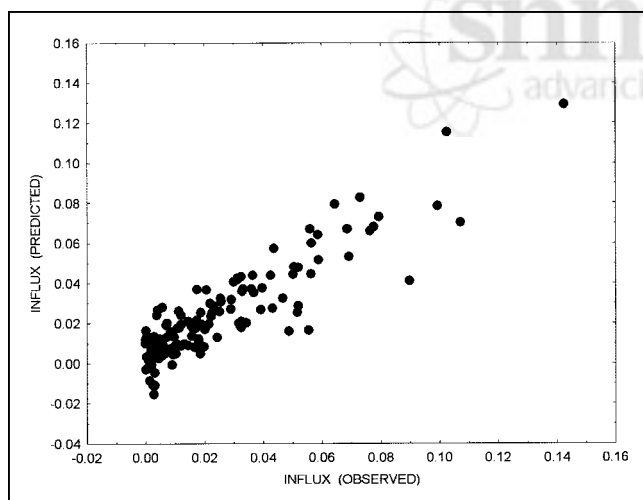


FIGURE 1. Correlation of ^{18}F -FDG influx as calculated by 2-compartment model (influx [observed]) and predicted influx (influx [predicted]) using short acquisition protocol. Dynamic input data from 1 to 10 min (10 frames) and target area from 1 to 10 min (10 frames) and from 56 to 60 min (1 frame) were used for prediction, based on polynomial function (degree 2) for data fitting. Correlation coefficient of 0.9028 was obtained.

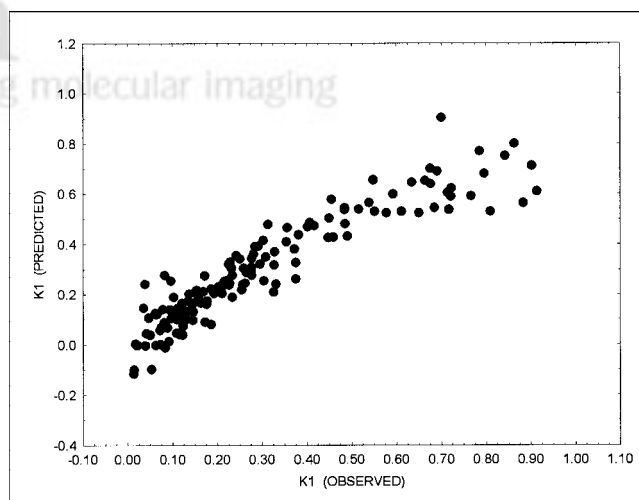


FIGURE 3. Correlation of k1 as calculated by 2-compartment model (k1 [observed]) and predicted k1 (k1 [predicted]) using short acquisition protocol. Input data from 1 to 10 min (10 frames) and target area from 1 to 10 min (10 frames) and from 56 to 60 min (1 frame) were used for prediction, based on polynomial function (degree 2) for data fitting. Correlation coefficient of 0.9305 was obtained.

(82.4%) and a higher specificity (92.9%). Their results demonstrated that the use of kinetic data enhances the diagnostic accuracy of ^{18}F -FDG PET.

The correlation between ^{18}F -FDG kinetics and tumor grading was evaluated in soft-tissue sarcomas (5). Again, the results showed that mainly grade III tumors could be differentiated when a compartment analysis of the ^{18}F -FDG data was used. By limiting the complexity of the data evaluation, calculation of global influx may help to improve diagnostic results. The authors showed that influx is a discriminant variable for grade III sarcomas and for lipomas and inflammatory lesions (5). Therefore, use of the influx as a parameter for routine diagnostic approaches in oncologic patients would be helpful.

PET follow-up examinations were performed on patients undergoing chemotherapy to assess response or nonresponse. However, because of the prolonged scanning time, it is difficult to perform dynamic studies on these patients routinely. Therefore, shortened procedures that provide information about the ^{18}F -FDG kinetics are needed. Our results showed that a short, 10-min, acquisition followed by a late static image 56–60 min after tracer injection provided accurate data for estimating ^{18}F -FDG influx and the parameters k_1 and VB . The initial 10-min data acquisition can be obtained immediately after the ^{18}F -FDG injection, and the patient can then be removed from the PET system. However, a general limitation of dynamic studies is the need to focus on a single target area because of the limited field of view of current PET scanners. Therefore, appropriate a priori information must be available to select the target region for the dynamic data acquisition, particularly for multifocal disease. This is especially important in patients who are evaluated for treatment response, in order to obtain data from the same anatomic region when follow-up studies are performed. If multiple lesions are present, one can use a modified whole-body protocol consisting of a short dynamic acquisition over the target area, which is most important for therapy management, followed by additional multiple bed positions using static acquisitions with short emission/transmission measurements to detect other possible lesions.

In most cases, the patient will be repositioned after 1 h to acquire the late scan for the dynamic evaluation, and additional bed positions will be used to obtain a partial body scan. Repositioning is a possible source of error for quantitative evaluation; therefore, skin markers must be used to maximize accuracy. To minimize error, a second transmission scan should be obtained. Through the use of iterative reconstruction methods for both emission and transmission data, the time for the transmission scan can be reduced up to 3–5 min. Repositioning errors in the reconstructed images should be taken into consideration when the data are evaluated, and if errors are present, the ROIs for the quantitative evaluation must be adjusted accordingly. Based on our PET system and the procedure used, the repositioning error is less than 2 cross-sections (slice thickness, 2.4 mm) in most patients when early and late images are compared.

Positioning of the patient in the PET system for tracer injection and initial data acquisition requires some changes in patient management. In our opinion, patients should be selected for the shortened dynamic protocol if a more detailed quantitative analysis of ^{18}F -FDG kinetics will likely be helpful for differential diagnostics or for assessment of the response to chemotherapy. In our experience, dynamic data can be helpful for differentiating soft-tissue sarcomas by grade (5). SUV was accurate in detecting grade III tumors (positive predictive value, 92%) but detected only 50% of grade I tumors. The kinetic data, in contrast, were helpful in the detection of 80% of grade I tumors and 84% of grade III tumors, as well as 50% of lipomas and 38% of grade II tumors. Furthermore, bone tumors may provide diagnostic difficulties, and kinetic data can help to differentiate benign from malignant lesions more accurately (15,16). Response to chemotherapy should be evaluated on the basis of dynamic PET studies to more accurately assess even small changes in ^{18}F -FDG kinetics. Our results indicate that a quantitative approach can improve the assessment of therapy response in patients with metastatic colorectal carcinoma (17,18).

Sugawara et al. used ^{18}F -FDG kinetic modeling in 21 patients with untreated and treated germ cell tumors (19). The major aim of the study was to evaluate the use of kinetic analysis for differentiating mature teratomas. The authors could differentiate viable tumors using the semi-quantitative SUV approach, but they did not find significant differences for mature teratomas and necrosis when SUV or visual analysis was used. In contrast, statistically significant differences were found for k_1 and for global ^{18}F -FDG influx (19). The results demonstrated that compartment analysis can provide additional information for the differentiation of tumors—information that cannot be obtained by visual analysis or static uptake measurements. We were able to show that, besides ^{18}F -FDG influx, VB and k_1 can also be estimated using the shortened acquisition protocol. With regard to the results of Sugawara et al., the shortened acquisition protocol and the estimation of k_1 from the dynamic data can be expected to be helpful in detecting and differentiating teratomas (19).

As shown by Sugawara et al., besides k_1 , the global ^{18}F -FDG influx (K_i), as calculated using the formula $K_i = (k_1 \times k_3)/(k_2 + k_3)$, also provides valuable information (19). In contrast to the compartment model, K_i can be calculated from a dynamic series using a graphical solution (20,21). Heiss et al. calculated the cerebral metabolic rate of glucose use in healthy human volunteers and noted a correlation to k_1 ($r = 0.88$) and k_3 ($r = 0.90$) (22). We noted lower correlation coefficients, probably because of the highly variable SUVs caused by the inclusion of various tumors as well as scar tissue, in contrast to the study of Heiss et al., who evaluated only normal brain structures. However, our results demonstrated that influx, k_1 , and VB can be estimated using the modified acquisition protocol.

The evaluation of dynamic PET studies can be especially helpful for assessing treatment effects. Avril et al. performed a prospective study on 73 patients with breast lesions suggestive of malignancy and performed a quantitative evaluation using the ^{18}F -FDG influx rate (23). The authors reported that the quantitative approach was helpful for differentiating benign from malignant lesions. Parametric imaging of the ^{18}F -FDG influx was performed by Zasadny and Wahl (24). They used a correlation coefficient-based filtering of the images and reported an enhancement of tumor-to-normal-tissue contrast for ^{18}F -FDG PET that may improve lesion detectability. Gupta et al. compared quantification with SUV and ^{18}F -FDG influx in patients with indeterminate lung lesions (4). Although a correlation existed between SUV and ^{18}F -FDG influx, the influx values were of additional clinical benefit in confirming a malignant or benign lesion in 3 patients with SUVs ranging from 2.0 to 2.39 (4). We noted a moderate correlation coefficient of 0.75 for the 56- to 60-min SUV and influx, which may be helpful for diagnosis but is of limited value for assessing response to treatment. Römer et al. performed dynamic PET studies with ^{18}F -FDG on patients with lymphoma and reported a larger change for influx data than for SUV (7). Indeed, according to our experience, influx data are more reproducible than is 60-min SUV and should be preferred. Even divergent results can be obtained for SUV and influx in some patients, as reported by Freedman et al. for a study on patients with renal cell carcinoma (25). These results direct to a more detailed analysis of PET data, which can be performed using the shortened acquisition protocol.

Several authors have attempted to solve the problem of the greater complexity of acquiring data for calculating ^{18}F -FDG influx, as compared with static SUV measurement. Minn et al. compared the 45- to 60-min postinjection SUV with the ^{18}F -FDG influx in 46 patients (26). They found a correlation coefficient of 0.91 for dose- and weight-normalized SUV and ^{18}F -FDG influx. The authors concluded that the single-scan SUV approach can be used for the assessment of ^{18}F -FDG uptake in tumors but that glucose concentration in blood must be monitored in patients with possible abnormalities of glucose metabolism. Actually, this limits the routine use of the SUV evaluation in oncologic patients. Suhonen-Polvi et al. reported a simplified quantification for the measurement of cerebral glucose use in children, using both an image-derived blood input curve and venous blood sampling for calculation of the metabolic rate (27). The authors found a correlation coefficient of 0.83 for SUV and the metabolic rate of glucose. Suhonen-Polvi proposed using the image-derived input function and 2–3 venous blood samples at the end of the study. SUV should be used as an alternative only if blood cannot be sampled. However, as already shown in the literature, input data can be retrieved from image data with high accuracy; therefore, blood sampling can be avoided (8). Sadato et al. performed ^{18}F -FDG studies on adults and proposed using the influx constant instead of SUV for diagnostic purposes (28). Again, they

sampled blood for up to 60 min, limiting the routine use of dynamic ^{18}F -FDG PET. Furthermore, a comparison with the full kinetic model was not done in that study.

Torizuka et al. used a short dynamic data acquisition for 0–30 min after ^{18}F -FDG injection (29). The authors applied a 2-compartment model to their data and calculated k_1 – k_3 . Interestingly, the rate constants were in excellent agreement with those obtained for 0–60 min. The lowest correlation, at $r = 0.886$, was observed for k_3 , giving evidence that the short acquisition protocol may be limited. How well a complete 2-compartment model, including VB and k_4 , will perform using the short dynamic acquisition was not shown. Our results show that, besides the influx constant, VB and k_1 can be estimated from the data. However, an input VOI is needed to improve the estimation of influx, VB, and k_1 . VB and k_1 were especially sensitive for the input data, and the use of target-area data alone limits the accuracy of the estimation.

CONCLUSION

The results show that a short dynamic data acquisition protocol can be used to obtain more detailed information about ^{18}F -FDG kinetics. ^{18}F -FDG influx, VB, and k_1 can be estimated from SUVs with high accuracy.

REFERENCES

1. Strauss LG, Conti PS. The applications of PET in clinical oncology. *J Nucl Med.* 1991;32:623–648.
2. Matthies A, Hickeys M, Cuchiara A, Alavi A. Dual time point ^{18}F -FDG PET for the evaluation of pulmonary nodules. *J Nucl Med.* 2002;43:871–875.
3. Hubner KF, Buonocore E, Gould HR, et al. Differentiating benign from malignant lung lesions using “quantitative” parameters of FDG PET images. *Clin Nucl Med.* 1996;21:941–949.
4. Gupta N, Harmindar G, Graeber G, Bishop H, Hurst J, Stephens T. Dynamic positron emission tomography with F-18 fluorodeoxyglucose imaging in differentiation of benign from malignant lung/mediastinal lesions. *Chest.* 1998;114:1105–1111.
5. Dimitrakopoulou-Strauss A, Strauss LG, Schwarzbach M, et al. Dynamic PET ^{18}F -FDG studies in patients with primary and recurrent soft-tissue sarcomas: impact on diagnosis and correlation with grading. *J Nucl Med.* 2001;42:713–720.
6. Nieweg OE, Pruijm J, van Ginkel RJ, et al. Fluorine-18-fluorodeoxyglucose PET imaging of soft-tissue sarcoma. *J Nucl Med.* 1996;37:257–261.
7. Römer W, Hanauske AR, Ziegler S, et al. Positron emission tomography in non-Hodgkin’s lymphoma: assessment of chemotherapy with fluorodeoxyglucose. *Blood.* 1998;12:4464–4471.
8. Ohtake T, Kosaka N, Watanabe T, et al. Noninvasive method to obtain input function for measuring glucose utilization of thoracic and abdominal organs. *J Nucl Med.* 1991;32:1432–1438.
9. Burger C, Buck A. Requirements and implementations of a flexible kinetic modeling tool. *J Nucl Med.* 1997;38:1818–1823.
10. Mikołajczyk K, Szabatin M, Rudnicki P, Grodzki M, Burger C. A Java environment for medical image data analysis: initial application for brain PET quantitation. *Med Inform.* 1998;23:207–214.
11. Miyazawa H, Osmond A, Petit-Taboue MC, et al. Determination of ^{18}F -fluoro-2-deoxy-D-glucose rate constants in the anesthetized baboon brain with dynamic positron tomography. *J Neurosci Methods.* 1993;50:263–272.
12. Sokoloff L, Smith CB. Basic principles underlying radioisotopic methods for assay of biochemical processes in vivo. In: Greitz T, Ingvar DH, Widén L, eds. *The Metabolism of the Human Brain Studied with Positron Emission Tomography.* New York, NY: Raven Press; 1983:123–148.
13. Strauss LG, Clorius JH, Kimmig B, et al. Imaging positron emitting radionuclides generated during radiation therapy. *Eur J Radiol.* 1989;9:200–202.
14. Haberkorn U, Ziegler SI, Oberdorfer F, et al. FDG uptake, tumor proliferation and expression of glycolysis associated genes in animal tumor models. *Nucl Med Biol.* 1994;21:827–834.

15. Dimitrakopoulou-Strauss A, Strauss LG, Heichel T, et al. The role of quantitative ^{18}F -FDG PET studies for the differentiation of malignant and benign bone lesions. *J Nucl Med.* 2002;43:510–518.
16. Wu H, Dimitrakopoulou-Strauss A, Heichel TO, et al. Quantitative evaluation of skeletal tumours with dynamic FDG PET: SUV in comparison to Patlak analysis. *Eur J Nucl Med.* 2001;28:704–710.
17. Dimitrakopoulou-Strauss A, Strauss LG, Rudi J. PET-FDG as predictor of therapy response in patients with colorectal carcinoma. *Q J Nucl Med.* 2003;47:8–13.
18. Dimitrakopoulou-Strauss A, Strauss LG, Rudi J, Burger C, Haberkorn U. Prediction of therapy outcome with FDG PET in metastatic colorectal cancer [abstract]. *J Nucl Med.* 2003;44(suppl):25P.
19. Sugawara Y, Zasadny KR, Grossman HB, Francis IR, Clarke MF, Wahl RL. Germ cell tumor; differentiation of viable tumor, mature teratoma, and necrotic tissue with FDG PET and kinetic modeling. *Radiology.* 1999;211:249–256.
20. Patlak CS, Blasberg RG. Graphical evaluation of blood-to-brain transfer constants from multiple-time uptake data: generalizations. *J Cereb Blood Flow Metab.* 1985;5:584–590.
21. Patlak CS, Blasberg RG, Fenstermacher JD. Graphical evaluation of blood-to-brain transfer constants from multiple-time uptake data. *J Cereb Blood Flow Metab.* 1983;3:1–7.
22. Heiss WD, Pawlik G, Herholz K, Wagner R, Goldner H, Wienhard K. Regional kinetic constants and cerebral metabolic rate for glucose in normal human volunteers determined by dynamic positron emission tomography of [^{18}F]-2-fluoro-2-deoxy-D-glucose. *J Cereb Blood Flow Metab.* 1984;4:212–223.
23. Avril N, Bense S, Ziegler SI, et al. Breast imaging with fluorine-18-FDG PET: quantitative image analysis. *J Nucl Med.* 1997;38:1186–1191.
24. Zasadny KR, Wahl RL. Enhanced FDG-PET tumor imaging with correlation-coefficient filtered influx-constant images. *J Nucl Med.* 1996;37:371–374.
25. Freedman NMT, Sundaram SK, Kurdziel K, et al. Comparison of SUV and Patlak slope for monitoring of cancer therapy using serial PET scans. *Eur J Nucl Med.* 2003;30:46–53.
26. Minn H, Leskinen-Kallio S, Lindholm P, et al. [^{18}F]fluorodeoxyglucose uptake in tumors: kinetic vs. steady-state methods with reference to plasma insulin. *J Comput Assist Tomogr.* 1993;16:115–123.
27. Suhonen-Polvi H, Ruotsalainen U, Kinnala A, et al. FDG-PET in early infancy: simplified quantification methods to measure cerebral glucose utilization. *J Nucl Med.* 1995;36:1249–1254.
28. Sadato N, Tsuchida T, Nakaumra S, et al. Non-invasive estimation of the net influx constant using the standardized uptake value for quantification of FDG uptake of tumours. *Eur J Nucl Med.* 1998;25:559–564.
29. Torizuka T, Nobeza S, Momiki S, et al. Short dynamic FDG-PET imaging protocol for patients with lung cancer. *Eur J Nucl Med.* 2000;27:1538–1542.

